9.1. PRINCIPLES OF MONOCHROMATIC DATA COLLECTION

spindle axis, as it can then never lie parallel to the beam. This can be a problem with cryogenic samples mounted in loops, where the preferred orientation is hard to dictate, and this is an example where a κ-goniostat is an advantage, allowing reorientation of the crystal.

Simplistic application of the above equation for estimating $\Delta\varphi$ is not receommended. The degree of overlap also depends on pixel size, beam cross section, crystal size and mosaicity, and crystal-to-detector distance. Given the influence of these additional parameters, it is in practice better to employ the integration software first to interpret the diffraction pattern and to simulate predicted patterns by adjusting the data-collection parameters. Several modern packages have such strategy features, and it is vital to employ them before collecting data. In fact, from a theoretical point of view, the highest signal-to-noise ratio is obtained when $\Delta\varphi$ corresponds to the rocking curve of the diffraction, *i.e.* the mosaic spread plus the beam divergence.

9.1.7. Rotation method: geometrical completeness

This topic has been reviewed by Dauter (2005).

9.1.7.1. Total rotation range for non-anomalous data

The total set of structure-factor amplitudes from a crystal is a sphere of points in reciprocal space, with a radius defined by the maximum resolution. The intensities of the two hemispheres of data show a centrosymmetric relationship based on Friedel's law, which only breaks down if anomalous scatterers are present. However, the diffraction pattern possesses internal symmetry related to that of the real-space unit cell. This means that for all space groups an asymmetric unit of reciprocal space can be defined. Provided the intensities of all reflections in this asymmetric unit have been measured, those of all others can be generated by the symmetry operations and the Fourier transform for the complete structure computed.

The asymmetric unit has the shape of a wedge extending from the origin at the centre of the reciprocal sphere with a cutoff at a maximum radius corresponding to the limiting diffraction angle (resolution). Once the Laue symmetry group of the crystal has been determined (*International Tables for Crystallography*, Volume A, 2005), it is straightforward to define the shape of this wedge and establish which data must be recorded to make up a complete unique set. For macromolecular crystals, where there can be no centre of symmetry, the possibilities are further simplified to the point group rather than the Laue group. All space groups belonging to the same point group have the same asymmetric unit. The only differences lie in the presence or absence of screw axes or centring. Thus, space groups $P2_12_12_1$, $P2_12_12$, $P222_1$, $P222$, $I222$ and $I2_12_12_1$ all belong to point group (symmetry class) 222 and have the same asymmetric unit in reciprocal space. The only consequence of the presence of screw axes or lattice centring is to introduce systematic absences for some classes of reflection within this asymmetric unit of the point group.

It is usual to define the limits of the asymmetric unit by placing restrictions on the indices. For point group 222, the common conventional choice of limits on the reflection indices hkl is

$$0 \leq h \leq h_{\max}, \qquad 0 \leq k \leq k_{\max} \qquad 0 \leq l \leq l_{\max},$$

where $h_{\max}$, $k_{\max}$ and $l_{\max}$ are defined by the maximum resolution. In all point groups, there are multiple but equivalent ways of defining the asymmetric unit, but a default definition is generally chosen by the data-reduction software. For example, in triclinic

symmetry, any hemisphere constitutes an asymmetric unit, and there are three typical choices of index limits:

$$0 \leq h \leq h_{\max}, \qquad \bar{k}_{\min} \leq k \leq k_{\max}, \qquad \bar{l}_{\min} \leq l \leq l_{\max},$$

or

$$\bar{h}_{\min} \leq h \leq h_{\max}, \qquad 0 \leq k \leq k_{\max}, \qquad \bar{l}_{\min} \leq l \leq l_{\max},$$

or

$$\bar{h}_{\min} \leq h \leq h_{\max}, \qquad \bar{k}_{\min} \leq k \leq k_{\max}, \qquad 0 \leq l \leq l_{\max}.$$

The standard choices of asymmetric unit taken from the *CCP4* program suite (Collaborative Computational Project Number 4, 1994) are shown in Table 9.1.7.1.

The data are complete if the Ewald sphere has been crossed by all reflections in the asymmetric part of the reciprocal lattice. During data acquisition and reduction, all measured indices are conventionally transformed to this asymmetric unit of reciprocal space. Firstly, this allows merging of symmetry-equivalent measurements as appropriate. Secondly, it allows the completeness of the data to be assessed efficiently, using contributions from the whole sphere.
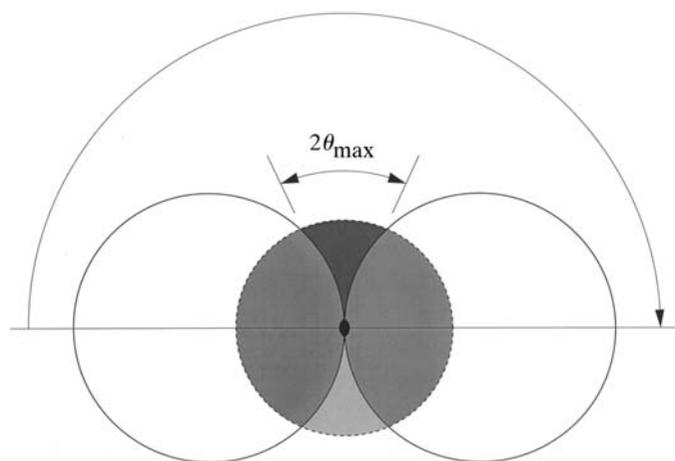
For all point groups, rotation of the crystal by 180° from any starting angle on the φ spindle axis is sufficient to provide a complete set of data (this is not sufficient if anomalous-dispersion measurements are required; see Section 9.1.7.2). Given such a total rotation, the redundancy of the measurements will increase with higher crystal symmetry. Thus, for a triclinic space group, the unique data will be measured almost twice on average (see the blind region below); for orthorhombic, eight times; for hexagonal class 6, 12 times; and for 622, 24 times. Redundancy is, in principle, advantageous, giving improved data quality (again see below), but it is generally possible to record complete unique data with a minimal overall rotation and correctly chosen starting angle on the spindle. It is of course necessary to determine the crystal orientation matrix, and this remains a vital part of the data-collection strategy. To minimize the effects of radiation

Table 9.1.7.1
Standard choice of asymmetric unit in reciprocal space for different point groups from the *CCP4* program suite

Point group	Index limits	
1	*hkl*:	$l \geq 0$
	*hk*0:	$h \geq 0$
	0*k*0:	$k \geq 0$
2	*hkl*:	$k \geq 0, l \geq 0$
	*hk*0:	$h \geq 0$
222	*hkl*:	$h \geq 0, k \geq 0, l \geq 0$
4	*hkl*:	$h \geq 0, k > 0, l \geq 0$
	0*kl*:	$k \geq 0$
422	*hkl*:	$h \geq k, k \geq 0, l \geq 0$
3	*hkl*:	$h \geq 0, k > 0$
	00*l*:	$l > 0$
321	*hkl*:	$h \geq k, k \geq 0$
	hhl:	$l \geq 0$
312	*hkl*:	$h \geq k, k \geq 0$
	*h*0*l*:	$l \geq 0$
6	*hkl*:	$h \geq 0, k > 0, l \geq 0$
	0*kl*:	$k \geq 0$
622	*hkl*:	$h \geq k, k \geq 0, l \geq 0$
23	*hkl*:	$h \geq 0, k > h, l > h$
	hkh:	$k \geq h$
432	*hkl*:	$h \geq 0, k \geq l, l \geq h$

Figure 9.1.7.1
Rotation of a triclinic crystal by 180° in the X-ray beam, represented as rotating the Ewald sphere with a stationary crystal, projected along the rotation axis. For the purpose of analysing the relation of data completeness to crystal symmetry and orientation the two representations are equivalent.
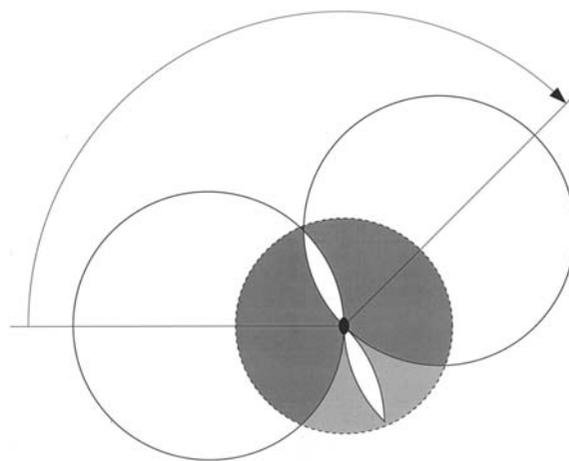
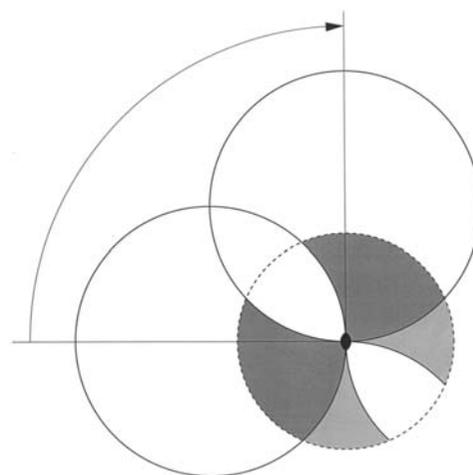

Figure 9.1.7.2
Rotation of a triclinic crystal by 135° is not sufficient to obtain totally complete data. At high resolution the completeness is higher than at low resolution, where a full 180° rotation is required.

damage, it is often beneficial to collect complete data with the minimal rotation range. This may well change with the advent of extremely fast detectors, when the decision-making process may take longer than data collection.

Thus, the crystal point-group symmetry has a profound effect on the total rotation range and the optimal starting spindle and crystal orientation for the most efficient recording of complete unique data. The rest of this section suggests strategies for the collection of complete data with minimal total rotation when anomalous-dispersion measurements are not required.

As stated above, for all crystals, rotation by 180° is sufficient to cover fully both sides of the Ewald sphere with intensity measurements. This is necessary for a triclinic crystal rotated around any arbitrary axis and also for a monoclinic crystal rotated around its unique b axis (Fig. 9.1.7.1). A twofold redundancy of unique data results; fourfold for the monoclinic case. Now consider a rotation of less than 180° (Fig. 9.1.7.2). Owing to the curvature of the Ewald sphere and the centre of symmetry arising from Friedel's law, the region of the sphere with reflections measured twice is diminished, and for part of the sphere there are no measurements. Most importantly, the proportions are resolution dependent. With a limited rotation, the high-resolution intensities reach a higher completeness than those at low resolution: data 90% complete at high resolution may be missing 20% of the low-resolution shells. Indeed, the low-resolution terms only become complete when a full 180° has been achieved.

The major data-processing software packages provide estimates of overall completeness as a function of total rotation range and starting point. However, they tend to neglect this variation with resolution. The fundamental importance of completeness at low resolution will be returned to later.

For total rotation by a given percentage of the angle needed to provide complete data, the resulting percentage completeness will be higher, again as a consequence of the curvature of the Ewald sphere. Consider again the triclinic case, when complete data require rotation by 180°. A single continuous range of 90° gives a completeness of about 65% (Fig. 9.1.7.3). Splitting the rotation range is advantageous; for example, if the crystal is rotated over two ranges of 45°, separated by a gap of 45°, the

completeness typically rises to about 80%. In summary, for the triclinic case, the starting point and crystal orientation are irrelevant, but if it is impossible to cover 180° in the time available, it is better to use two or more sets of ranges. The software can again often provide advice on such strategies.

When the crystal has symmetry elements, the situation is more complex. Now the completeness is sensitive to the starting point of rotation and the crystal orientation, as well as the total rotation range used. All three must be considered in defining an optimum strategy for minimal rotation to give complete data. Consider an orthorhombic unit cell where the asymmetric unit comprises any octant of the reciprocal lattice. Minimal complete data require a total rotation of 90° between any twofold axis and the plane perpendicular to it (Fig. 9.1.7.4). This requires that one of the major axes must lie along the direction of the beam, either at the start or end of the 90° rotation, when the other two axes will lie in the plane of the detector. It is not necessary to rotate around one of the major axes, but the rotation axis should lie in one of the three major planes. If these conditions on crystal orientation or starting point are not satisfied, then more than a 90° rotation will be required. The proper selection of starting point is vital. A 90°

Figure 9.1.7.3
After a 90° rotation out of a required 180°, the overall completeness is higher than 50%.
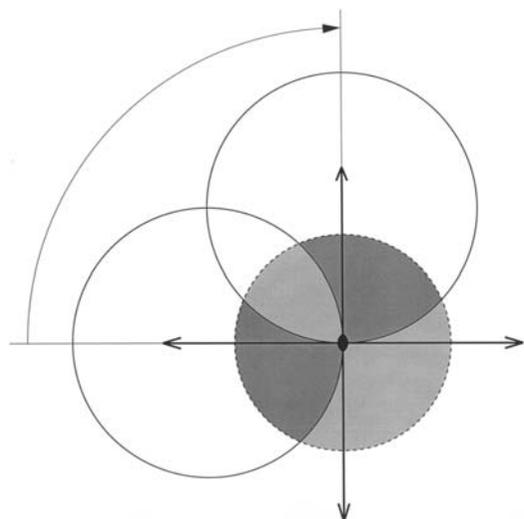
Figure 9.1.7.4
For an orthorhombic crystal, a 90° rotation is sufficient provided the starting or final orientation is along the major axis.

rotation starting midway between two axial positions, when the major axis only lies along the beam after 45°, will reduce the completeness after 90° to about 65%, since in essence the same 45° of unique data will be measured twice, albeit with high redundancy (Fig. 9.1.7.5). This emphasizes the need to define the crystal symmetry and orientation properly before data collection if minimalist protocols are to be employed.

In general, the higher the crystal symmetry, the more the completeness depends on the crystal orientation. In point groups 321 or 312, the asymmetric unit may be defined as a 30°-wide wedge that spans the space between the positive and negative direction of the threefold c axis. The index limits are

$$0 \leq h \leq h_{max}, \qquad 0 \leq k \leq h, \qquad \bar{l}_{max} \leq l \leq l_{max}.$$

If the crystal is mounted with the threefold axis along the rotation spindle, it is sufficient to rotate by 30°, but only if the a or b axis lies along the beam at the start or end of the range. In contrast, if the crystal is rotated around **a** or **b**, then it is necessary to cover 90°. The second procedure will lead to a threefold increase in redundancy, but at the expense of a longer time.

The total rotation requirements for various crystal symmetries and orientations are given in Table 9.1.7.2. It is difficult to give
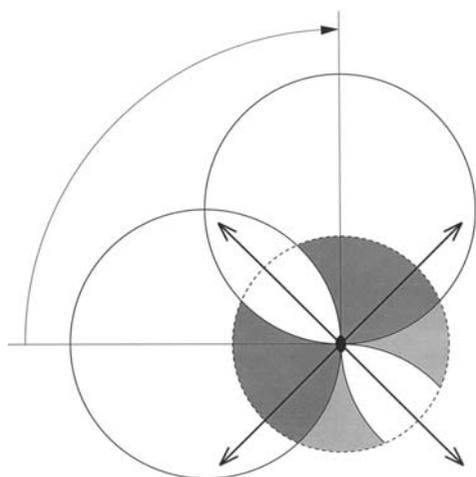
Figure 9.1.7.5
Rotation of an orthorhombic crystal by 90° between two diagonal orientations leaves a part of the reciprocal space unmeasured.

Table 9.1.7.2
Rotation range (°) required in different crystal classes

The direction of the spindle axis is given in parentheses; ac means any vector in the ac plane.

Point group	Native data	Anomalous data
1	180 (any)	$180 + 2\theta_{max}$ (any)
2	180 (b); 90 (ac)	180 (b); $180 + 2\theta_{max}$ (ac)
222	90 (ab or ac or bc)	90 (ab or ac or bc)
4	90 (c or ab)	90 (c); $90 + \theta_{max}$ (ab)
422	45 (c); 90 (ab)	45 (c); 90 (ab)
3	60 (c); 90 (ab)	$60 + 2\theta_{max}$ (c); $90 + \theta_{max}$ (ab)
32	30 (c); 90 (ab)	$30 + \theta_{max}$ (c); 90 (ab)
6	60 (c); 90 (ab)	60 (c); $90 + \theta_{max}$ (ab)
622	30 (c); 90 (ab)	30 (c); 90 (ab)
23	~60	~70
432	~35	~45

reliable estimations for cubic crystals, since then the requirements vary dramatically with the crystal orientation.

In the above, it was assumed that the detector was mounted centrally with respect to the incident X-ray beam. If it is offset either by a 2θ arm or by a translation, then the completeness for any total rotation range will be reduced. Software will generally be required to estimate the effective completeness and derive optimum strategies. For minimalist approaches to obtaining a high completeness, the importance of selecting the total rotation range, the optimal starting point and indeed the crystal orientation must be stressed. This means that the crystal orientation must be defined at the start of the experiment from the initial exposures.

9.1.7.2. Total rotation range for anomalous-dispersion data

In the presence of anomalous-scattering centres, Friedel's law breaks down and the intensities of the two halves of the reciprocal sphere are no longer equivalent. Strictly speaking, reflections related by a centre of symmetry or mirror relation cease to have equal intensities, but those related by pure rotation preserve their equivalence. The non-equivalent pairs of reflections are known as Bijvoet pairs. In macromolecular crystallography, it is often highly desirable to record the intensity differences between the Bijvoet mates to provide information on the position of anomalous scatterers, usually to be exploited in phasing procedures (Part 14). The anomalous signal should also be retained for so-called native data, for example in the discrimination between water and ions in the surface solvent shell.

This implies that the intensities of the unique reflections have to be measured for both hemispheres of reciprocal space. In the general (triclinic) case, this requires the rotation of the crystal by a wider rotation range. At very low resolution, the surface of the Ewald sphere can be approximated by a plane. In this case, rotation of the lower half of the Ewald sphere will cover a full hemisphere of data, and the upper half will cover the remaining centrosymmetrically related hemisphere. At high resolution, the surface of the Ewald sphere increasingly deviates from planarity by the Bragg angle θ on each side (Fig. 9.1.7.6). To record complete anomalous data for such a triclinic crystal therefore requires it to be rotated by $180° + 2\theta_{max}$ from a random starting position. This will measure each Bijvoet mate at least once. However, only after a total rotation of 360° will the average multiplicity reach a value of two.

Similar reasoning applies to higher-symmetry space groups. Intensity data for two asymmetric units related by a centre of
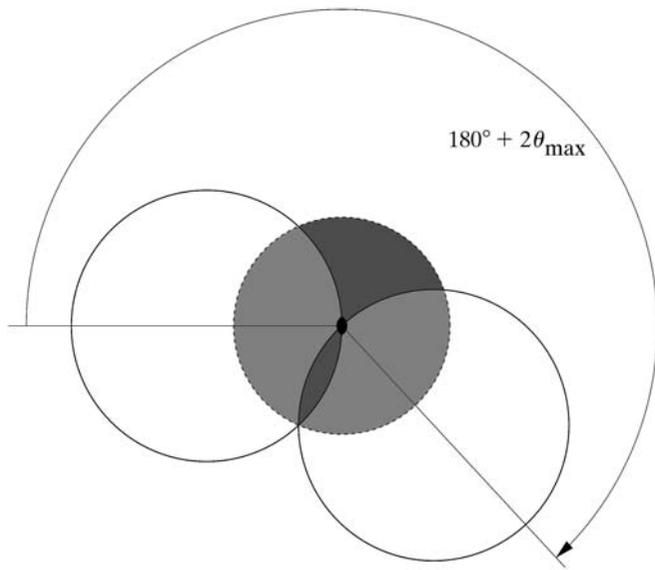
Figure 9.1.7.6
For data containing an anomalous signal, when both Bijvoet mates have to be measured, 180° rotation of a triclinic crystal is not sufficient and at least an additional $2\theta_{max}$ is required.

symmetry or a mirror need to be recorded. For some cases, the total range remains the same for completeness of anomalous data as for native. However, in several symmetries or orientations, the total range must again be increased by either θ_{max} or $2\theta_{max}$ (Table 9.1.7.2).
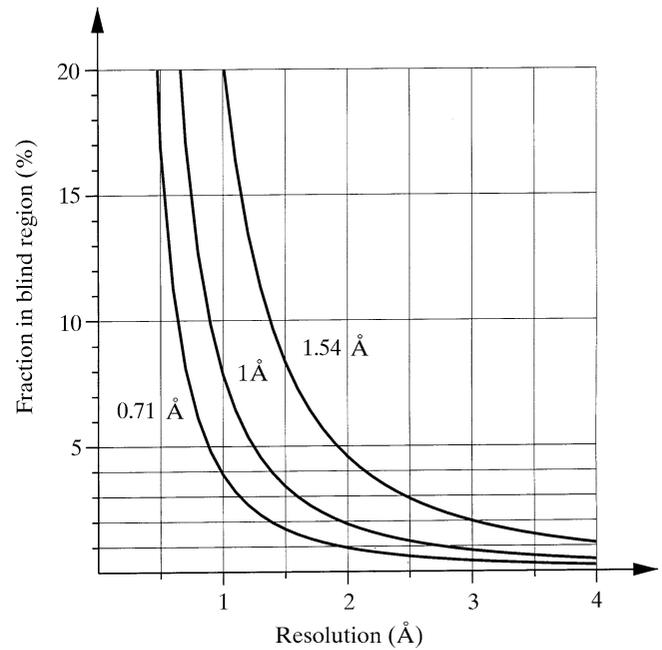
9.1.7.3. Blind region

Even after rotation of the crystal about a single axis by 360°, some reflections do not cross the surface of the Ewald sphere and cannot be measured. These lie in a cusp around the rotation axis which is referred to as the blind region. This is in principle a disadvantage of the single-rotation method, but for most systems the problems are easily overcome. Owing to the curvature of the Ewald sphere, the width of the blind region increases with the resolution and directly depends on a single parameter, the diffraction angle θ (Fig. 9.1.7.7). The fraction, B_θ, of unrecordable reflections lying in the blind region at a particular resolution with
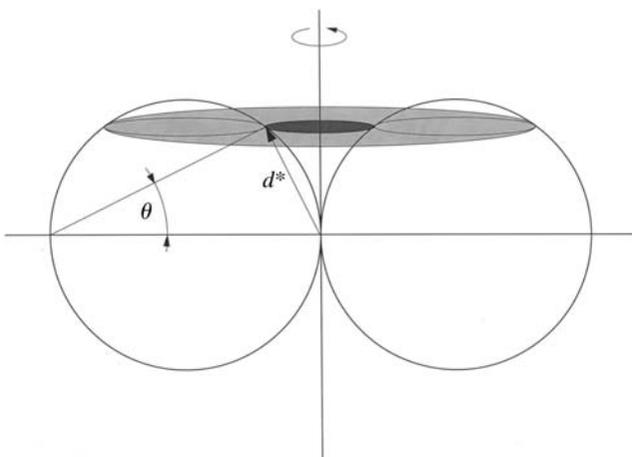
Figure 9.1.7.7
Rotation by 360° leaves the part of the reciprocal space in the blind region unmeasured, since the reflections near the rotation axis do not cross the surface of the Ewald sphere. The rotation axis in this projection lies vertically in the plane of the figure.

Figure 9.1.7.8
Dependence of the total fraction of reflections in the blind region on the resolution for three different wavelengths: 1.54, 1 and 0.71 Å.

Bragg angle θ is given by

$$B_\theta = 1 - \cos\theta.$$

The cumulative fraction, B_{tot}, of reflections in the blind region up to a certain resolution is given by

$$B_{tot} = 1 - 3(4\theta - \sin 4\theta)/(32\sin^3\theta).$$

B_{tot} is shown graphically as a function of resolution for selected wavelengths in Fig. 9.1.7.8.

For a particular resolution limit, the blind region is narrower if the wavelength is short, since the surface of the Ewald sphere is flatter (Fig. 9.1.7.9). This is an advantage of using short-wavelength radiation. For Cu $K\alpha$ radiation at 2.0 Å resolution, the blind region amounts to less than 5%. With shorter wavelengths, it falls below 2%.

The two halves of the blind region on either side of the Ewald sphere are related by the centre of symmetry. In the triclinic case, the blind region is therefore unavoidable with a single mount of
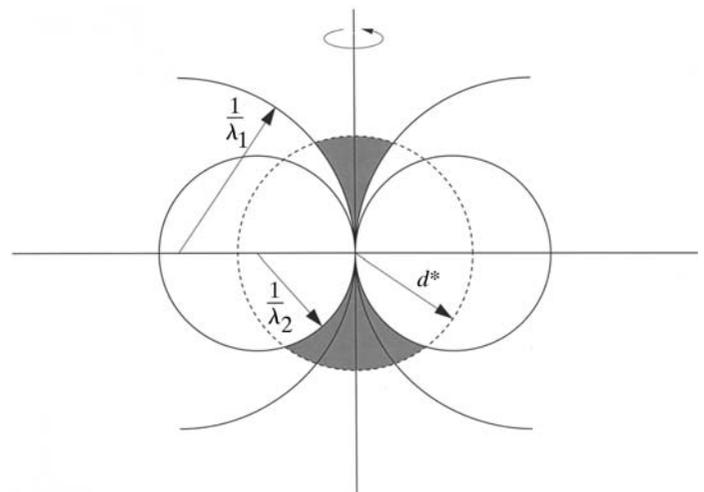
Figure 9.1.7.9
For shorter wavelengths the blind region is narrower, since the Ewald sphere is flatter.
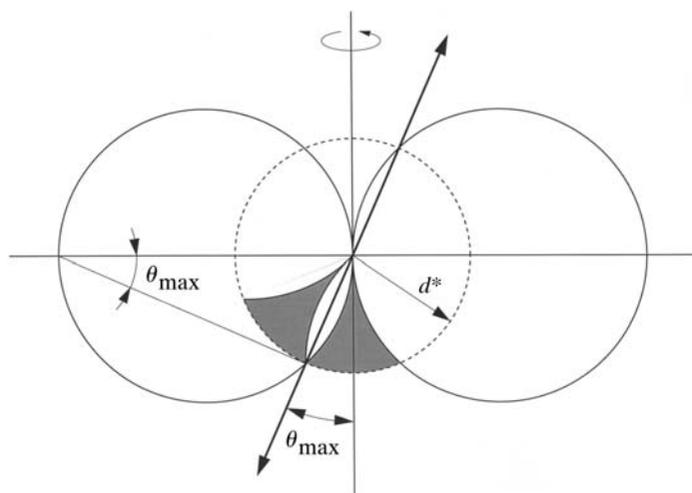
Figure 9.1.7.10
If the crystal has a symmetry axis, it should be skewed from the rotation axis by at least θ_{max} to be able to collect the reflections equivalent to those in the blind region.

the crystal. The only solutions are to use a second mount of the crystal offset by at least 2θ from the first, easily achievable with a κ-goniostat, or to measure from a second sample.

For crystals with symmetry higher than $P1$, reflections that are symmetry-equivalent to those in the blind region may be recorded, and there will be no loss of unique reflections. Only if the unique axis passes through the blind region approximately parallel to the spindle axis will the reflections lying close to it not be repeated by symmetry in another region of reciprocal space. To avoid the blind region, it is sufficient to misorient the unique symmetry axis by at least θ_{max} from the rotation axis (Fig. 9.1.7.10). To achieve full completeness, monoclinic crystals should not be oriented along the unique twofold axis or along any vector in the *ac* plane.

The reciprocal-lattice points on the border of the blind region cross the surface of the Ewald sphere at a very acute angle or fail to cross it completely, staying in the diffracting position for a considerable time. Their intensity cannot be measured accurately, because the Lorentz factor is large and its magnitude is very sensitive to minor errors in the orientation matrix. These reflections are located on the detector window along the line parallel to the spindle axis and should not be integrated.

The detrimental effect of the blind region on the completeness of data is negligible at medium and low resolution or if the crystal is non-axially oriented. This means that a simple single rotation axis is sufficient for the majority of applications.

9.1.7.4. Alternative indexing

If the crystal point-group symmetry is lower than the symmetry of its Bravais lattice, then the reflections can be indexed in more than one way. In other words, the symmetry of the reflection positions is higher than the symmetry of the distribution of their intensities. This situation typically arises for point groups with polar axes, such as groups 3, 4 or 6, which can be indexed with the *c* axis pointing in either one of two directions. The lattice does not define the directionality of such axes if its two remaining cell dimensions are equivalent. This problem does not occur in the monoclinic system, despite the polar twofold axis, as the two other axes are not equivalent. The most complex case is point group 3, which can be indexed in the 622 lattice in four non-equivalent ways. The other such groups have only two alternatives.

Table 9.1.7.3
Space groups with alternative, non-equivalent indexing schemes

Symmetry operations required for re-indexing are given as relations of indices and in the matrix form. In brackets are the chiral pairs of space groups indistinguishable by diffraction. These space groups may also display the effect of merohedral twinning, with the twinning symmetry operators the same as those required for re-indexing.

Space group	Re-indexing transformation	
$P4$, $(P4_1, P4_3)$, $P4_2$, $I4$, $I4_1$	$hkl \rightarrow kh\bar{l}$	$010/100/00\bar{1}$
$P3$, $(P3_1, P3_2)$	$hkl \rightarrow \bar{h}\bar{k}l$	$\bar{1}00/0\bar{1}0/001$
	or $hkl \rightarrow kh\bar{l}$	$010/100/00\bar{1}$
	or $hkl \rightarrow \bar{k}\bar{h}l$	$0\bar{1}0/\bar{1}00/00\bar{1}$
$R3$	$hkl \rightarrow kh\bar{l}$	$010/100/00\bar{1}$
$P321$, $(P3_121, P3_221)$	$hkl \rightarrow \bar{h}\bar{k}l$	$\bar{1}00/0\bar{1}0/001$
$P312$, $(P3_112, P3_212)$	$hkl \rightarrow \bar{h}\bar{k}l$	$\bar{1}00/0\bar{1}0/001$
$P6$, $(P6_1, P6_5)$, $(P6_2, P6_4)$, $P6_3$	$hkl \rightarrow kh\bar{l}$	$010/100/00\bar{1}$
$P23$, $P2_13$, $(I23, I2_13)$, $F23$	$hkl \rightarrow k\bar{h}l$	$010/\bar{1}00/001$

There is an analogous problem for cubic space groups within point group 23. Here the lattice possesses fourfold symmetry, but the intensity distribution has only twofold symmetry. Rotation by $90°$ leads to alternative, although perfectly permitted, indexing of reflections.

Each allowed scheme is permitted and self-consistent for a single crystal, since all possibilities will perfectly match the crystal lattice. However, under alternative indexing schemes, the same reflection will be given different indices, which can pose problems when data from more than one crystal are to be merged or compared. Merging is needed when more than one sample is required to record a complete data set. Comparison is needed when looking for heavy-atom derivatives or for ligand complexes with isomorphous crystals. For these, the reflections of one crystal must be selected as a standard, and it is easy to make other crystals consistent with this standard either by changing the orientation matrix at the time of intensity integration or by applying re-indexing to the integrated intensity set. The alternative indexing schemes are related by those symmetry operations present within the higher symmetry of the Bravais lattice but absent from the point-group symmetry. The point groups with alternative indexing systems are shown in Table 9.1.7.3, together with the necessary symmetry operations for re-indexing.

Several experiments require the recording of multiple data sets from the same crystal. One example is the collection of more than one pass with different exposure times (see below), and a second is in multiwavelength anomalous dispersion (MAD) experiments. In these experiments, the software systems may independently choose any of the alternative systems for different sets, which may then be incompatible and need re-indexing. It is much simpler to ensure a common orientation matrix modified as appropriate for all sets at the time of intensity integration.

9.1.8. Crystal-to-detector distance

The crystal-to-detector distance (CTDD) should be selected so that the whole area of the detector is usefully exploited. The shorter the CTDD, the higher the resolution of the indexed reflections at the edge of the image; but if the CTDD is too short, then the outer regions of the detector window record only indices with attached noise rather than intensities. A longer CTDD spreads the background radiation over a larger area of the detector as the background level diminishes in proportion to the square of the CTDD. In contrast, owing to collimation and focusing, the profiles of the Bragg reflections do not broaden so

references